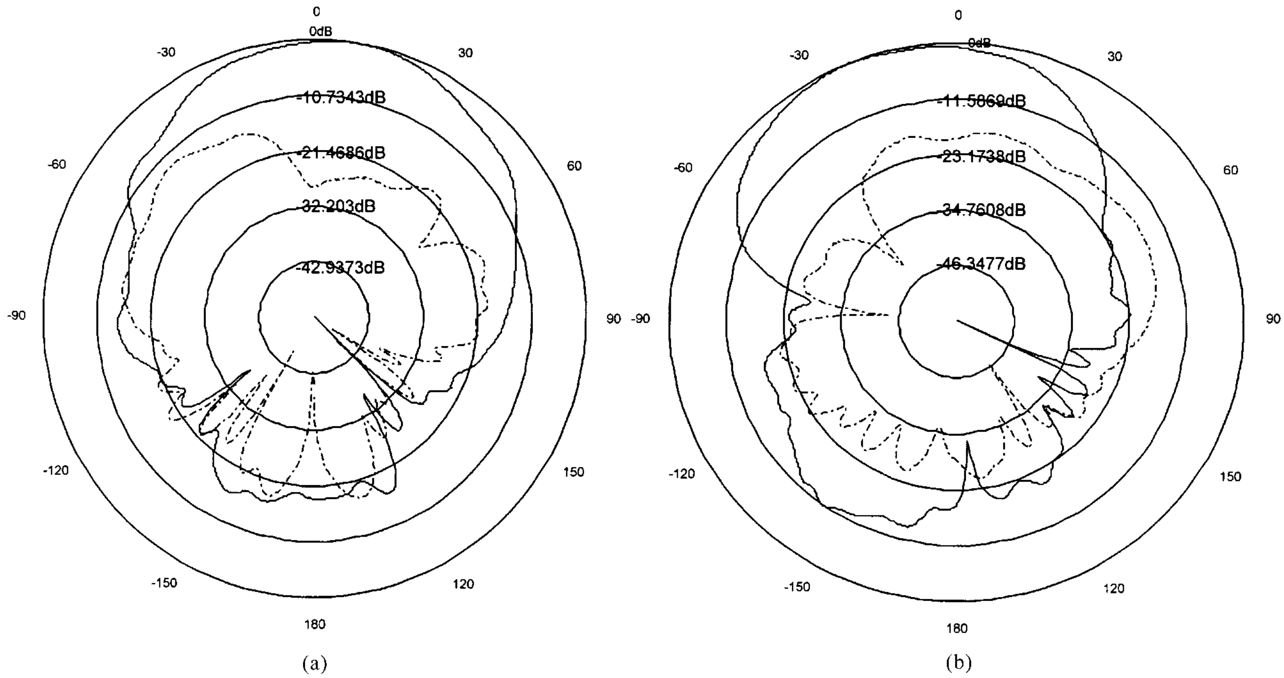

Figure 7 Radiation pattern of the conventional dual-stacked patch antenna measured at 11 GHz. (a) Solid line: E-plane copolarization; dotted line: E-plane cross polarization. (b) Solid line: H-plane copolarization; dotted line: H-plane cross polarization

communications where, very often, a large bandwidth is desired.

REFERENCES

1. D.M. Pozar, A microstrip antenna aperture coupled to a microstripline, Electron Lett 21 (1985), 49–50.
2. S.D. Targonski, R.B. Waterhouse, and D.M. Pozar, Design of wide-band aperture-stacked patch microstrip antennas, IEEE Trans Antennas Propagat 46 (1998), 1245–1251.
3. J.F. Zuircher, The SSFIP: A global concept for high performance broadband planar antennas, Electron Lett 24 (1988), 1433–1435.
4. Y. Mushiake, Self-complementary antennas, IEEE Trans Antennas Propagat 34 (1992), 23–29.

THREE-DIMENSIONAL MODELING OF ETCHED GROOVE SEPARATION OF ADJACENT OPTICAL WAVEGUIDES

Husain M. Masoudi[1] and Samir J. Al-Bader[1]
[1] Department of Electrical Engineering
King Fahd University of Petroleum and Minerals
Dhahran, Saudi Arabia

Received 17 June 1999

ABSTRACT: *Using the three-dimensional explicit finite-difference beam propagation method, we investigate the effect of placing an etched groove in the region separating the two rib waveguides of a directional coupler. The purpose of the groove is to inhibit channel interaction. We concentrate on the calculation of the groove depth necessary for channel isolation. We also show that the application of the groove can be accompanied by a small power loss.* © 1999 John Wiley & Sons, Inc. Microwave Opt Technol Lett 23: 289–291, 1999.

Key words: *optical waveguides; 3-D modeling; integrated optics; beam propagation*

I. INTRODUCTION

Many of the important integrated optical devices depend on the interaction of adjacent channels for their operation. In most cases, the interaction takes place over precisely determined lengths as in directional couplers, switches, and modulators. Beyond these lengths, proper operation requires that the interaction be terminated. This requirement is usually satisfied by bending the channels away from each other. An alternative technique for channel isolation based on the abrupt introduction of etched grooves (slots) in the space between the channels has recently been proposed [1]. In comparison to bends and S-bends, this technique has the advantages of compactness (no extra lateral subspace space) and abruptness of action. Using a slab model with the assumption of etched grooves can lead to the complete isolation of adjacent channels with very small power loss caused by radiation.

In this work, we address the question of groove depth, and show that isolation is obtained with a groove depth on the order of 1 μm for the structure at hand. We use the three-dimensional explicit finite-difference beam propagation method (EFD–BPM) [2–4] to follow the evolution of the optical field in a symmetric directional coupler made of two adjacent rib waveguides with a groove of finite depth etched in the middle of the spacer region. We also show that the introduction of the groove results in a very small power loss. The choice of the method of analysis (EFD–BPM) has been made because of its simplicity, efficiency, and particular suitability to the problem at hand [3–4].

II. NUMERICAL METHOD

Starting with the scalar parabolic equation for a three-dimensional field ϕ

$$2jk_o n_o \frac{\partial \phi}{\partial z} = \frac{\partial^2 \phi}{\partial x^2} + \frac{\partial^2 \phi}{\partial y^2} + k_o^2(n^2 - n_o^2)\phi \qquad (1)$$

where n_o is a reference refractive index, k_o is the free-space wave number, and $n(x, y, z)$ is the refractive index, and using the central finite-difference approximations for the partial derivatives leads to the discrete EFD equation [2–4]

$$\begin{aligned}\phi_{i,m}(z + \Delta z) &= \phi_{i,m}(z - \Delta z) + a_x[\phi_{i-1,m}(z) + \phi_{i+1,m}(z)] \\ &\quad + a_y[\phi_{i,m-1}(z) + \phi_{i,m+1}(z)] + b_{i,m}\phi_{i,m}(z) \quad (2)\end{aligned}$$

where $b_{i,m} = (\Delta z/jk_o n_o)[k_o^2(n_{i,m}^2 - n_o^2) - 2/\Delta x^2 - 2/\Delta y^2]$, $a_x = \Delta z/(jk_o n_o \Delta x^2)$, and $a_y = \Delta z/(jk_o n_o \Delta y^2)$. i and m represent the discretization of the transverse coordinates x and y, respectively, while Δx and Δy are the transverse mesh sizes, and Δz is the longitudinal step size. Equation (2) is stable if $\Delta z < 2k_o n_o/[(4/\Delta x^2) + (4/\Delta y^2) + k_o^2|n_{i,m}^2 - n_o^2|_{\max}]$. On the other hand, the EFD–BFM is very efficient because marching the input field one propagational step requires multiplication with a very sparse matrix that contains only five nonzero elements in each row [2].

III. RESULTS

Figure 1 shows a cross-sectional view of the directional coupler structure used in the computation. In the following analysis, the first guided mode of the isolated rib waveguide of Figure 1 has been used as an input. We use the power spectral method to calculate the mode effective index and the field distribution from the BPM field [5]. With the structure of Figure 1 without an etched groove ($D_g = 0$), we also calculate, using the spectral method, the coupling length of the directional coupler by computing the mode indexes of the even (N_{eff}^*) and the odd (N_{eff}^o) modes. The cross-coupling length is found to be $L_c = \lambda/2(N_{\text{eff}}^e - N_{\text{eff}}^o) = 6.5$ mm, where λ is the wavelength. All of the results appearing in this work are made with $\Delta x = \Delta y = 0.1$ μm and $\Delta z = 0.0275$ μm with zero field boundary condition at the edge of the computational window. The parameters of Figure 1 indicate that the modes of the rib waveguides are strongly confined. We have used a large computational window to minimize the influence of the zero field at its edge. Figure 2 shows contour plots of the field for the power exchange between the two waveguides without a groove ($D_g = 0$) at several propagational distances.

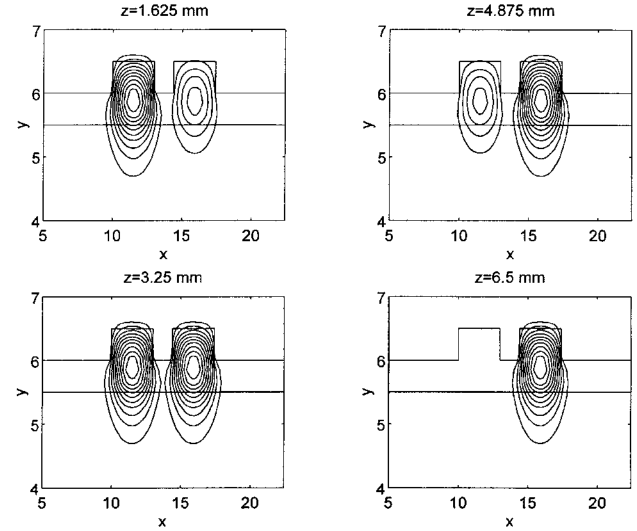

Figure 2 Field contours showing the power exchange between the two arms of the directional coupler of Figure 1 in the absence of an etched groove ($D_g = 0$) at several propagational distances

The input field (not shown) is the mode of the isolated left waveguide of Figure 1 applied at $z = 0$. The profile of this field is very similar to the one shown in the last plot (at $z = 6.5$ mm). Figure 3 shows the same variables as in Figure 2, but with an etched groove of depth $D_g = 1$ μm in the middle of the space between the two waveguides. The etched groove is introduced into the structure at $z = 0$. The action of the etched groove in isolating the waveguides is clearly demonstrated. The power introduced into the left waveguide is seen to remain in this channel because of the action of the groove. In Figure 4, we show the transmissivity of the left and right channels. The computation of the normalized intensities has been carried out numerically by evaluating the square of the magnitude of the projected total BPM field onto the normalized input mode, and then normalizing with respect to the input intensity. Figure 4 shows the normalized intensities as a function of propagation distance for several groove depths. It is seen that, as the groove depth increases, the interaction length between the two waveguides increases. For

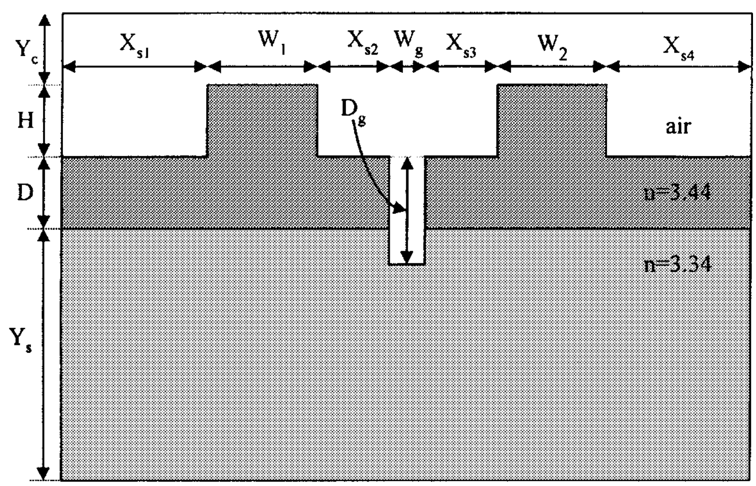

Figure 1 Cross-sectional view of the directional coupler structure with an etched groove of depth D_g placed symmetrically between the two rib waveguides. The parameters used in the analysis are: $Y_s = 5.5$, $D = 0.5$, $H = 0.5$, $Y_c = 0.5$, $X_{s1} = X_{s4} = 10.0$, $W_1 = W_2 = 3.0$, $X_{s2} = X_{s3} = 0.5$, $W_g = 0.4$, and a wavelength of 1.55 (all dimensions are in micrometers)

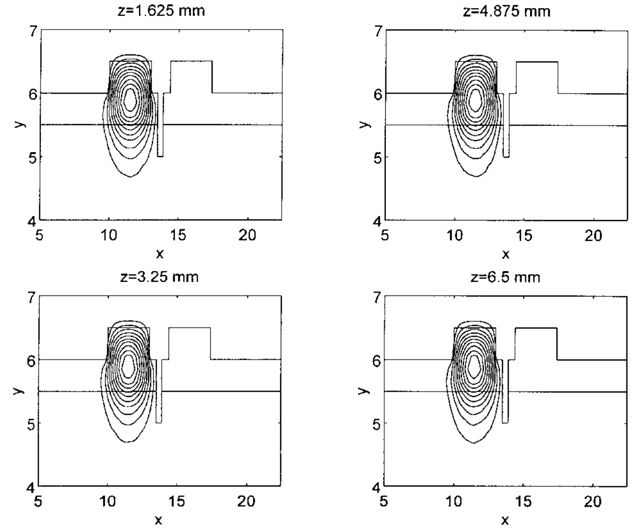

Figure 3 Same as Figure 2, but with an etched groove of $D_g = 1$ μm at several propagational distances.

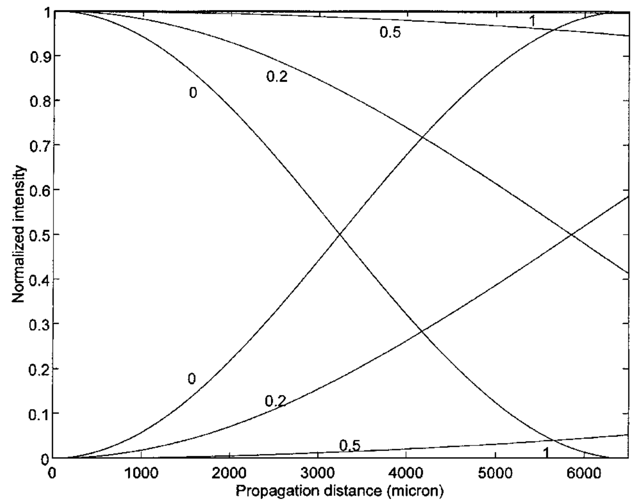

Figure 4 Normalized intensities of the left and right channel fields during the course of propagation for several groove depths. Curves starting from 1 belong to the left waveguide where the input is applied, and curves starting from 0 belong to the right waveguide. The numbers on the curves represent the groove depth D_g in micrometers.

a sufficiently deep groove (≈ 1 μm for the above structure), the interaction between the two waveguides can be considered to be negligible. It is also observed that the power loss in the presence of a deep groove is negligible for the structure investigated.

IV. CONCLUSION

A very effective technique for isolating adjacent optical channel waveguides has been demonstrated by using the explicit finite-difference BPM. It has been found that etching a groove of a finite depth in the space between interacting waveguides can inhibit the exchange of power between them. This action is obtained abruptly, in contrast to waveguide bends. The particular advantages of the etched groove are compactness and low power loss.

ACKNOWLEDGMENT

The support of King Fahd University of Petroleum and Minerals, Dhahran, Saudi Arabia is gratefully acknowledged.

REFERENCES

1. S.J. Al-Bander, Application of etched grooves in integrated-optics channel isolation, IEEE Photon Technol Lett 8 (1996), 1044–1046.
2. Y. Chung and N. Dagli, Analysis of Z-invariant and Z-variant semiconductor rib waveguides by explicit finite difference beam propagation method with nonuniform mesh configuration, IEEE J Quantum Electron 27 (1991), 2296–2305.
3. H.M. Masoudi and J.M. Arnold, Parallel three-dimensional finite-difference beam propagation methods, Int J Numer Modeling 27 (1995), 95–107.
4. H.M. Masoudi and J.M. Arnold, Modeling second-order nonlinear effects in optical waveguides using a parallel-processing beam propagation method, IEEE J Quantum Electron 31 (1995), 2107–2113.
5. M.D. Feit and J.A. Fleck, Computation of mode eigenfunctions in graded index optical fibers by the propagating beam method, Appl Opt 19 (1980), 2240–2246.

CCC 0895-2477/99

THE NOVEL ARCHITECTURES OF SMART OPTOELECTRONIC LOGIC CIRCUITS BASED ON DIRECTIONAL COUPLERS

Wen-Ching Chang,[1] Yang-Han Lee,[1] and Jiang-Duh Fang[1]
[1] Department of Electrical Engineering
Tamkang University
Tamsui, Taipei Hsien, Taiwan 25137, R.O.C.

Received 2 June 1999

ABSTRACT: *Novel architectures of the smart optoelectronic logic gate and SR flip-flop are proposed for the first time. In the former, both the AND and OR functions can be integrated in a single circuit. These optoelectronic circuits are composed of integrated optical waveguide directional couplers, optoelectronic converters, EDFAs, a delay line, and a DFB laser. Importantly, linear device operation with low power is the main advantage as compared to the conventional optoelectronic logic elements. Moreover, the characteristics of these optoelectronic circuits, such as optical path, slew-rate limiting, and phase retardation on the different states of operation, are discussed and are found to be informative.* © 1999 John Wiley & Sons, Inc. Microwave Opt Technol Lett 23: 291–294, 1999.

Key words: *optoelectronic logic circuit; flip-flop; erbium-doped fiber amplifier; directional coupler*

1. INTRODUCTION

In recent years, optoelectronic logic gates and flip-flops (FF) have attracted much research and stimulated great development in high-speed integrated optical systems [1–5]. In 1988, Awwal and Karim proposed a JK FF by using a polarization-encoded optical shadow-casting (POSC) algorithm [1]. Following the bistable technique, much research that focused on photonic FF logic operations has been completed successfully [2–5]. Lentine et al. reported a photonic set–reset latch which was accomplished with the symmetric self-electro-optic effect device (S-SEED) by using the quantum-confined Stark